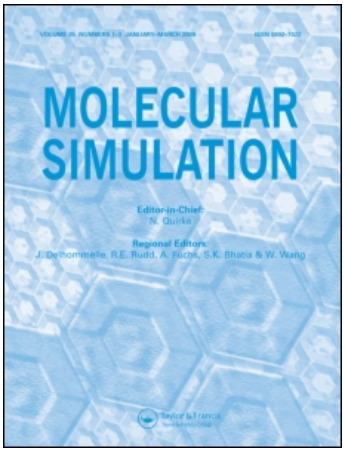

Molecular Simulation
Publication details, including instructions for authors and subscription information:
http://www.informaworld.com/smpp/title~content=t713644482

Gigahertz frequency tuner based on a telescoping double-walled carbon nanotube: molecular dynamics simulations

Jeong Won Kang[a]; Ki Ryang Byun[b]; Oh Kuen Kwon[c]; Young Gyu Choi[a]; Ho Jung Hwang[b]
[a] Department of Computer Engineering, Chungju National University, Chungju, Republic of Korea [b] School of Electrical and Electronic Engineering, Chung-Ang University, Seoul, Republic of Korea [c] Department of Electronic Engineering, Semyung University, Jecheon, Republic of Korea

Online publication date: 11 May 2010

To cite this Article Kang, Jeong Won , Byun, Ki Ryang , Kwon, Oh Kuen , Choi, Young Gyu and Hwang, Ho Jung(2010) 'Gigahertz frequency tuner based on a telescoping double-walled carbon nanotube: molecular dynamics simulations', Molecular Simulation, 36: 6, 418 — 424
To link to this Article: DOI: 10.1080/08927020903544543
URL: http://dx.doi.org/10.1080/08927020903544543

Molecular Simulation
Vol. 36, No. 6, May 2010, 418–424

Taylor & Francis
Taylor & Francis Group

Gigahertz frequency tuner based on a telescoping double-walled carbon nanotube: molecular dynamics simulations

Jeong Won Kang[a], Ki Ryang Byun[b], Oh Kuen Kwon[c], Young Gyu Choi[a] and Ho Jung Hwang[b]*

[a]*Department of Computer Engineering, Chungju National University, Chungju 380-702, Republic of Korea;* [b]*School of Electrical and Electronic Engineering, Chung-Ang University, Seoul 156-756, Republic of Korea;* [c]*Department of Electronic Engineering, Semyung University, Jecheon 390-711, Republic of Korea*

(*Received 11 August 2009; final version received 9 December 2009*)

The schematics of a gigahertz-range tuner is addressed as an application of a telescoping multi-walled carbon nanotube (CNT) that can be used repeatedly, and its dynamic operation is investigated via classical molecular dynamics simulations based on a (5,5)(10,10) double-walled CNT. Fine control of the telescoped length of the double-walled CNT enables its resonance frequency to be matched to one of the signal frequencies, and the telescoped nanotube can be tuned to its resonance frequency for use as a component of a bandpass filter.

Keywords: nanotube tuner; nanotube resonator; molecular dynamics

PACS: 61.46.+ w; 66.30.Pa; 83.10.Rs

1. Introduction

Carbon nanotubes (CNTs) [1] have recently attracted a great deal of attention, because their mechanical and electrical properties are ideal for nanoelectromechanical systems (NEMSs) [2,3]. Multi-walled CNTs, which consist of multiple, precisely nested concentric nanotubes, exhibit a striking telescoping property, where an inner nanotube core can slide across the atomically smooth casing of an outer nanotube shell [4]. This property has been exploited to build a rotational nanomotor [5] and nanorheostat [6]. Future nanomachines such as gigahertz mechanical oscillators are envisioned [7]. Several types of CNT-based NEMSs have already been demonstrated, such as gigahertz oscillators [8–13], data storage nanodevices [14], nanotweezers [15] and random access memory [16]. There has been progress in analysing and constructing nanotube-based resonators [13,17,18].

Recently, Jensen et al. [18] introduced tunable resonators based on CNTs that operate at a single frequency or have a relatively narrow frequency range. However, these properties may limit their application. By exploiting the versatile telescoping property of multi-walled CNTs, they created a tunable nanoscale resonator operating at frequencies up to 300 MHz, which is tunable over a range of more than 100 MHz. Relatively high-quality factors (up to 1000) indicated that the sliding friction between telescoping sections of the resonator was an insignificant source of dissipation, and telescoping increased quality factors via the suppression of thermo-elastic dissipation. Jensen et al. [19] also introduced a nanotube radio that consisted of an antenna and a tuner, via a cantilevered single-walled CNT. By controlling the length of the cantilevered single-walled CNT, the nanotube's resonance frequency matched the transmitted carrier wave frequency, the nanotube was resonated and the radio reception occurred. However, their cantilevered nanotube tuners were used once for all because the nanotube was continuously shortened by the trimming process.

In this work, we introduce the schematics of a nanotube tuner operating in the gigahertz range. It is based on a telescoping tunable resonator that can be used repeatedly, which is composed of a multi-walled CNT. We perform classical molecular dynamics (MD) simulations for a telescoped double-walled CNT resonator, and show that a telescoping nanotube is applicable to a filter or a tuner in the gigahertz range.

2. Schematics

Figure 1(a) shows the simple schematics of a telescoping double-walled CNT-based gigahertz tunable resonator. By controlling the bias of the gate electrode, the telescoped cantilevered CNT can be vibrated as studied in the previous work [18,19], and then the vibrating CNT tip can be detected by the anode electrode [19]. When we want to change the vibrating frequency of the CNT tip, the desired frequency can be achieved by changing the length of the vibrating CNT by manipulating the *XY* position controller. Higher frequencies are achieved by moving back the *XY*

*Corresponding author. Email: hjhwang@cau.ac.kr

ISSN 0892-7022 print/ISSN 1029-0435 online

DOI: 10.1080/08927020903544543
http://www.informaworld.com

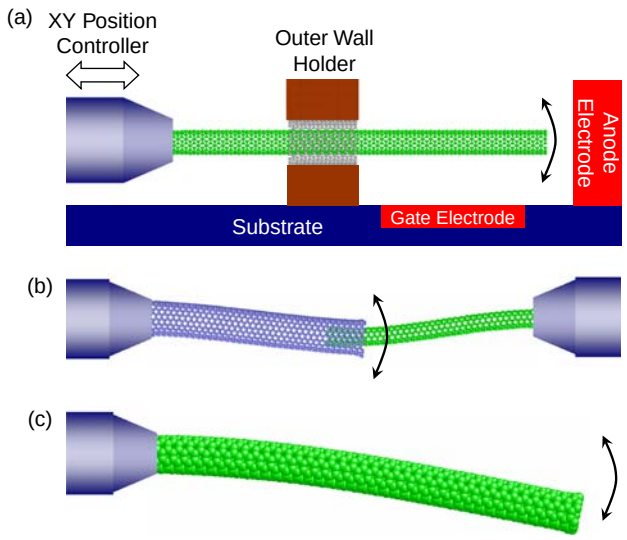

Figure 1. (a) Simple schematics of a telescoping double-walled CNT-based gigahertz tunable resonator. (b) Simple schematics of the previous CNT-based tunable resonator [18]. (c) Simple schematics of the previous cantilevered single-walled CNT tuner in the nanotube radio [19].

position controller whereas lower frequencies are achieved by approaching the *XY* position controller.

Our tunable CNT resonator is different from the previous CNT-based tunable resonators described by Jensen et al. [18,19]. They created a tunable nanoscale resonator by exploiting the versatile telescoping property of multi-walled CNTs as shown in Figure 1(b) [18]. Both sides of the multi-walled CNT were clamped and one side of them was connected to a position controller to achieve a telescoped CNT. Frequency bandwidth of our cantilevered-type design can be greater than that of the bridged type. They also introduced the cantilevered single-walled CNT tuner in the nanotube radio that was tuned via a two-step process as shown in Figure 1(c) [19]. First, there is a trimming process, which is terminated when the nanotube's resonance frequency is within the target frequency band. Second, fine-tuning of the radio within the desired band is accomplished by tensioning the nanotube with an electrostatic field. Therefore, their cantilevered nanotube tuners had a one-time usage, because the nanotube was continuously shortened by the trimming process. However, the telescoping nanotube tuner in our design can be used repeatedly, because a telescoped nanotube can be restored to the initial position. The tunable bandwidth can be controlled by adjusting the length of the multi-walled CNT.

3. Methods

The MD code was the same as that used in our previous works [20–25], where we used the velocity Verlet algorithm, a Gunsteren–Berendsen thermostat to control the temperature and neighbour lists to improve the computing performance. The MD time step was 5×10^{-4} ps. The initial velocities were derived from the Maxwell distribution, and the magnitudes were tuned to ensure that the temperature in the system remained constant. In all MD simulations, the temperature was constant at 1 K, and it was controlled via a Gunsteren–Berendsen thermostat. In order to calculate interatomic interactions, we used two empirical potential functions. For carbon–carbon interactions, we used the Tersoff–Brenner potential function [26–28], which has been widely used for carbon systems. The long-range interactions of carbon were characterised via the Lennard-Jones 12-6 (LJ12-6) potential, via the parameters given in Mao et al. [29]. The parameters for the LJ12-6 potential were $\varepsilon_C = 0.0042$ eV and $\sigma_C = 3.37$ Å. The cut-off distance of the LJ12-6 potential was 10 Å.

A nanotube-based tuner was investigated via classical MD simulations, and we used a double-walled CNT consisting of (5,5), with a length of 7, 10 or 11.5 nm, and a (10,10) CNT, with a length of 1, 2 or 3 nm. Figure 2 shows an atomic structure of a double-walled CNT tuner used in the simulations. In Figure 2, the lengths of the inner and outer CNTs are denoted by L_T and L_O, respectively, and the length of the actually oscillating CNT is denoted by L_R. The length of the CNT connected with the *XY* position controller is denoted by L_M. It was assumed that the left end of the (5,5) CNT would be connected to the externally controlled system and the outer wall would be combined with the outer wall holder, as shown in Figure 1(a). So, the atoms composed of the (10,10) CNT and the left boundary atoms of the (5,5) CNT remained fixed in the MD simulations. The MD simulations of the other atoms were based on constraint dynamics at a constant temperature. The left end of the (5,5) CNT was telescoped by $\delta = 1$ nm. In order to obtain the resonance frequencies, MD simulations of the initial

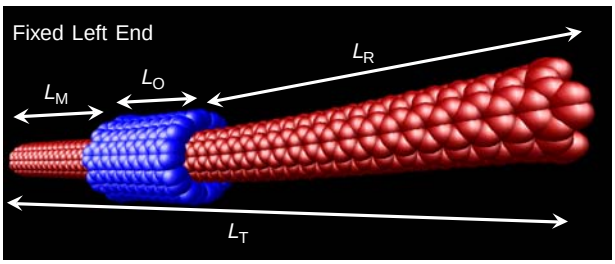

Figure 2. An atomic structure of a double-walled (5,5)(10,10) CNT tuner used in the simulations. The lengths of the inner and outer CNTs are denoted by L_T and L_O, respectively, and the length of the actually oscillating CNT is denoted by L_R. The length of the CNT connected with the *XY* position controller is denoted by L_M.

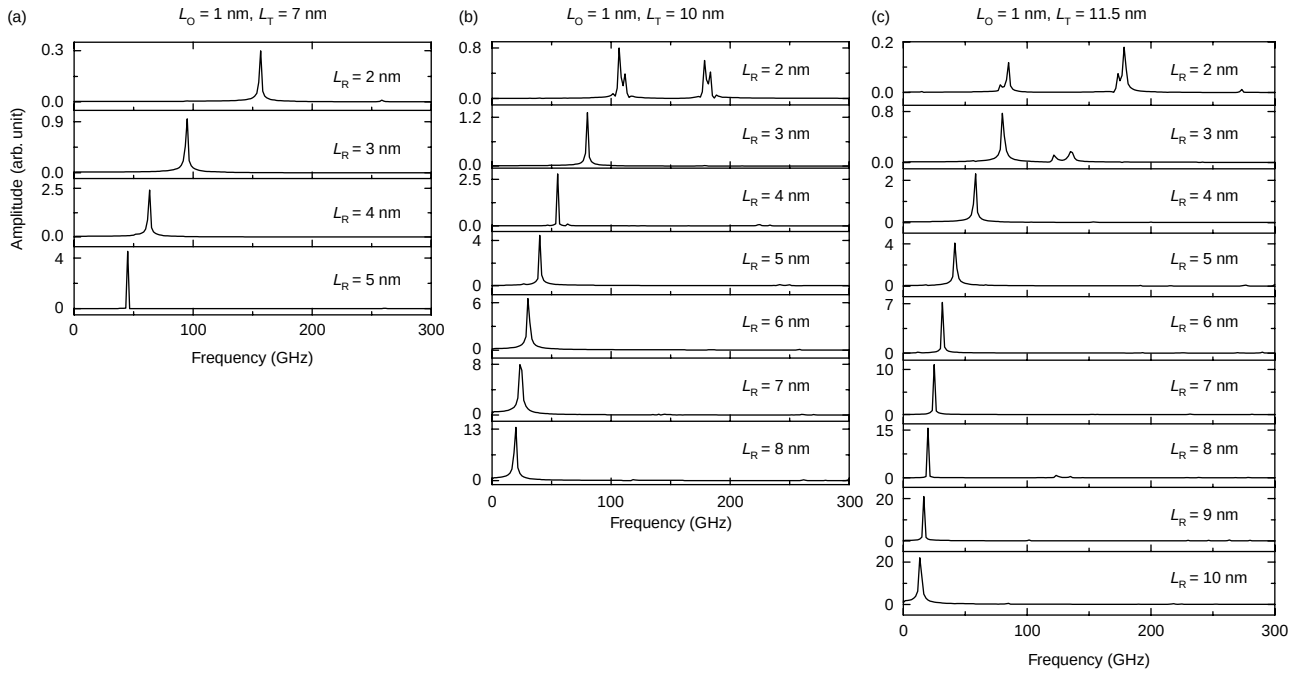

Figure 3. Amplitude spectra vs. frequency for $L_O = 1$ nm. $L_T =$ (a) 7, (b) 10 and (c) 11.5 nm.

external force during the initial 2.5 ps were performed, and then, upon the removal of the bending force, the CNT resonators were left to oscillate freely, and, finally, the resonance frequencies (f) were analysed via the fast Fourier transform using the data obtained from the MD simulations for 500 ps.

4. Results and discussion

The amplitude spectra vs. frequency are plotted in Figures 3–5 for $L_O = 1$, 2 and 3 nm, respectively. Figures 3–5(a)–(c) show the spectra as a function of L_R for $L_T = 7$, 10 and 11.5 nm for the corresponding L_O, respectively. The spectra explicitly show a trend between

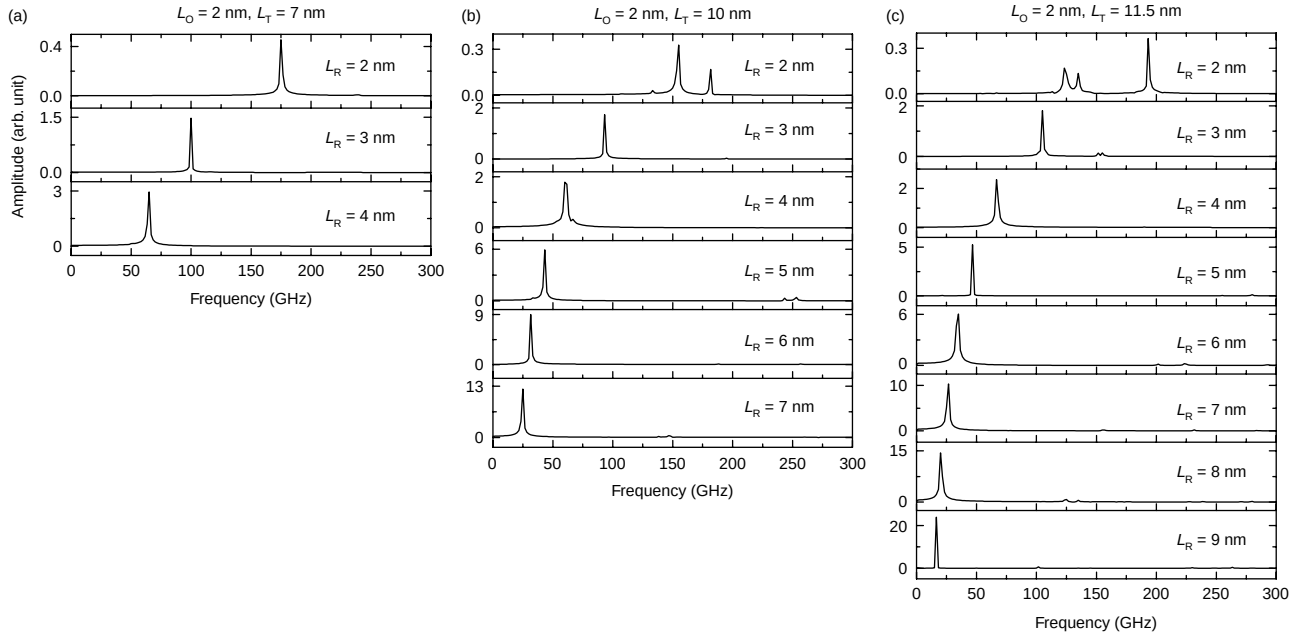

Figure 4. Amplitude spectra vs. frequency for $L_O = 2$ nm. $L_T =$ (a) 7, (b) 10 and (c) 11.5 nm.

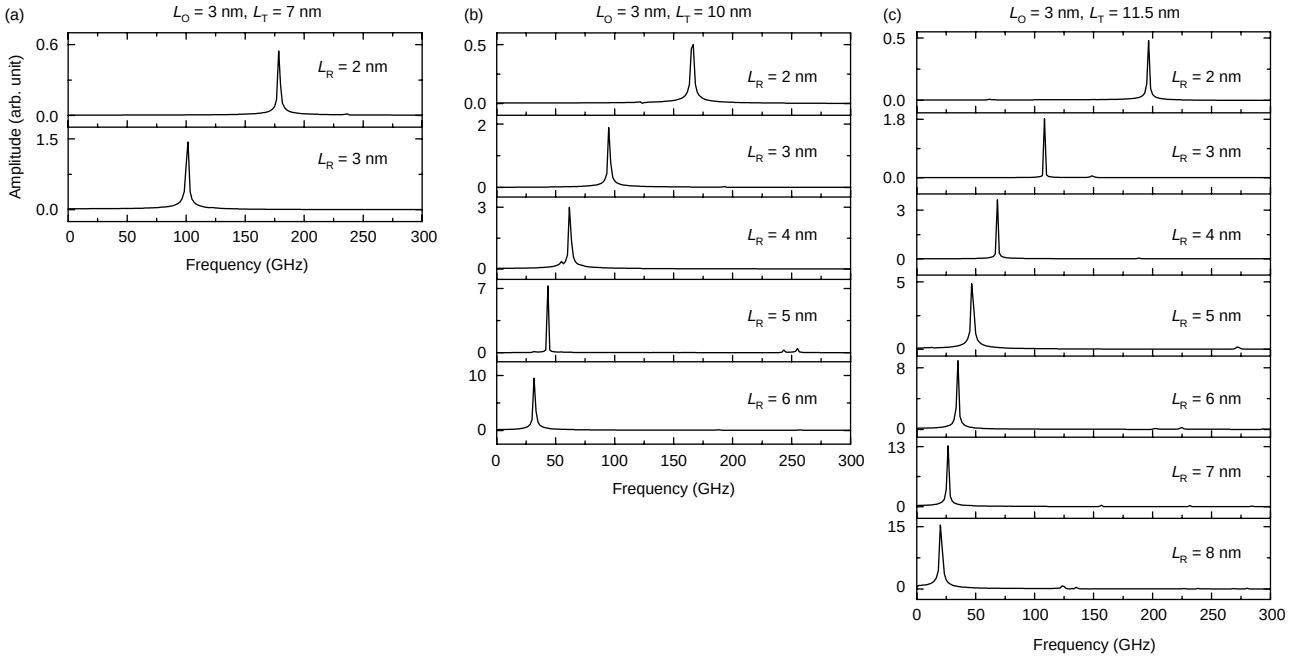

Figure 5. Amplitude spectra vs. frequency for $L_O = 3$ nm. $L_T =$ (a) 7, (b) 10 and (c) 11.5 nm.

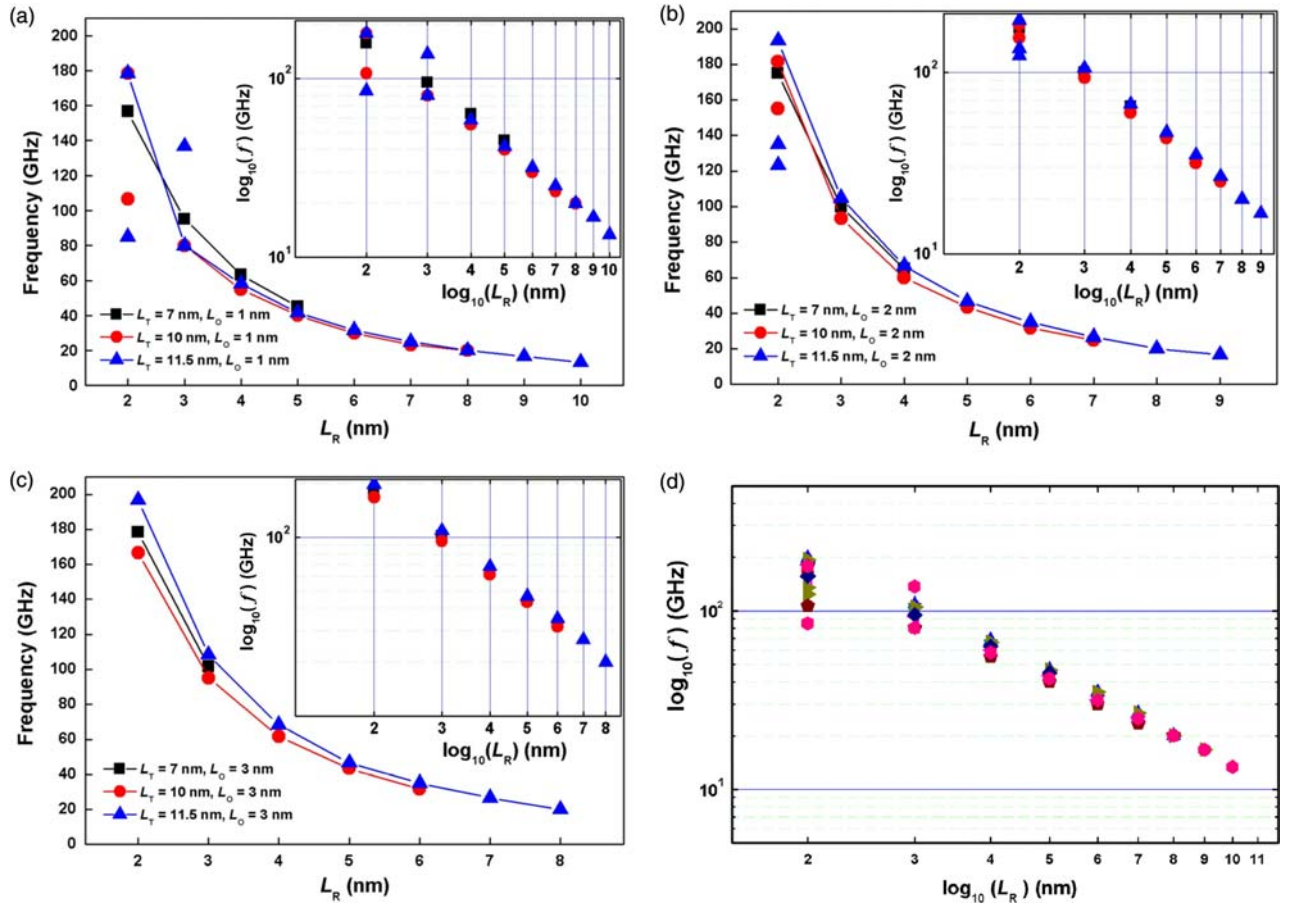

Figure 6. Frequencies (f_R) corresponding to the main peaks are plotted as a function of L_R. The plots (a)–(c) are for Figures 3–5, respectively. The insets are the $\log_{10}(f_R)$–$\log_{10}(L_R)$ plots. (d) f_R–L_R plots in the log–log scales using all data obtained from (a)–(c).

the main peaks and L_R. Frequencies (f_R) corresponding to the main peaks are plotted as a function of L_R in Figure 6(a)–(c), which are for Figures 3–5, respectively. The insets of Figure 6(a)–(c) show the $\log_{10}(f_R)$–$\log_{10}(L_R)$ plots.

Although the f_R–L_R plots in Figure 6 have the same slope regardless of the L_O, the different L_T results in the slight difference of f_R for the same L_R. As the length of the L_R decreases, the difference increases. The reason for this is that the oscillation of the left side with a length of the L_M affects the oscillation of its active region with a length of the L_R. Therefore, we can find that, in some spectra, with $L_R = 2$ nm, as shown in Figures 3(b)–(c) and 4(b)–(c), we can find some minor peaks beside the main peak. The vibrations of the L_M regions can be found in Figure 7, which shows the motions of the telescoped CNT resonators for four cases such as $L_R = 8$, 6, 4 and 2 nm for the tunable resonator, with $L_T = 11.5$ nm and $L_O = 2$ nm. As the length of the L_R decreases, the length of the L_M increases; therefore, the increasing length of the L_M makes for the left region of the CNT to decrease its vibrational frequency. The low-frequency vibration of the L_M region affects the high-frequency vibration of the L_R region. Therefore, the decreasing oscillation of the left region with the L_M induces the damping effect of the vibration of the active region with the L_R. The oscillation of the left region with the L_M with lower frequency must be correlated with the oscillation of the right region with the L_R. Therefore, some of the cases with $L_R = 2$ or 3 nm appear as minor peaks induced by coupling motions. Long outer wall for the L_O can act as a blocking wall against the wave propagation of the L_M region; hence, the vibration of the active region with the L_R can be independent of the vibration of the left region with the L_M because of the long outer wall for the L_O. Therefore, the length of the outer wall can be carefully selected to obtain a reliable tuner.

Figure 6(d) shows the f_R–L_R plots in the log–log scales using all data obtained from Figure 6(a)–(c). As discussed above, for the cases with $L_R = 2$ and 3 nm, the corresponding frequencies are widely scattered. However, as the L_R increases, the corresponding fundamental frequencies are the same with each other regardless of the L_T. The frequencies are well fitted by a power function, $f = 509L_R^{-1.615}$, and this relationship closely coincides with that found in previous experiments [18,19] and simulations [30].

In general, the tension in the telescoped multi-walled CNT resonator was influenced by the vdW attraction between the core and outer nanotubes, and the tension remained constant, regardless of the length, temperature or other environmental factors [18]. For double-walled CNTs, the tension was also constant, regardless of the length, whereas the vdW interaction energy was dependent on the length [7]. However, in our model, the tension

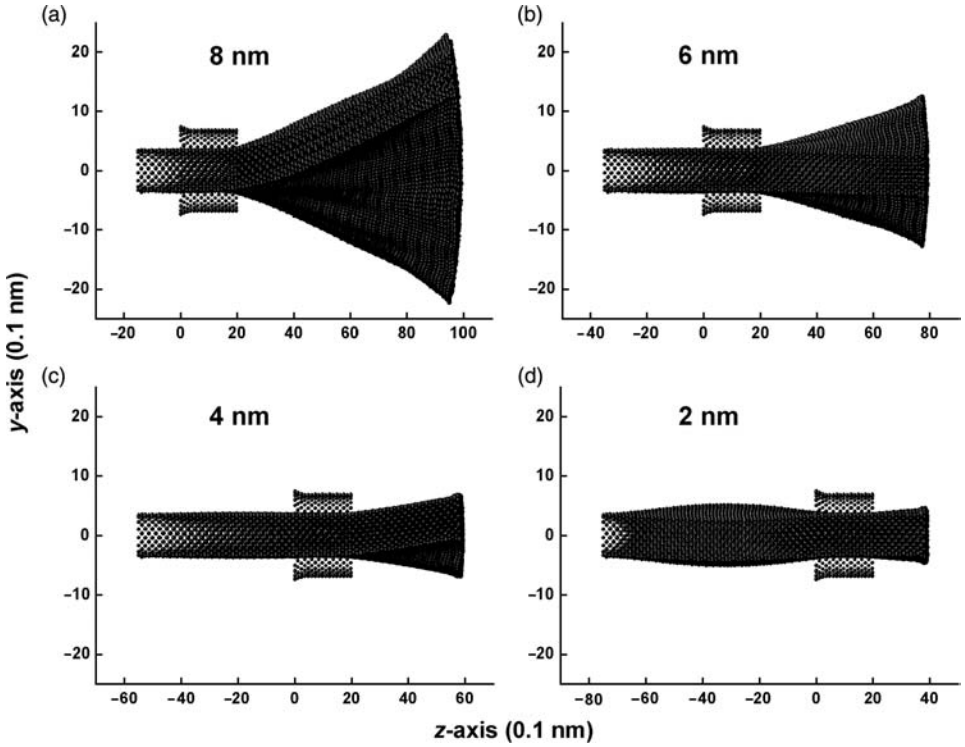

Figure 7. Motions of the telescoped CNT resonators for four cases such as L_R = (a) 8, (b) 6, (c) 4 and (d) 2 nm for the tunable resonator, with $L_T = 11.5$ and $L_O = 2$ nm.

induced by the vdW interaction between the core and the outer nanotubes is almost zero and not sensitive to the operation of the telescoping tunable CNT resonator because the vdW attractions are induced by both sides of the outer wall, as shown in Figures 1 and 2, and both tensions are balanced. The vdW energy between the core and the outer nanotubes remains constant regardless of the telescoping length. However, the energy dissipation of the telescoping tunable CNT resonator is closely related to the length of the telescoped double-walled CNTs. As the length of the telescoped multi-walled CNTs increased, the rate of kinetic energy dissipation increased [18]. The sensitivity of the mechanical beam oscillator, which usually operates at its harmonic resonance frequency in practical applications, is largely dependent on the quality factor Q (the inverse of the energy dissipation) of the oscillator. However, the maximum external potential energy is reduced to $E_{\text{ext}} - \Delta E_{\text{ext}}$ at the conclusion of each oscillation cycle, due to energy loss or damping, where E_{ext} and $-\Delta E_{\text{ext}}$ represent the external potential energy and energy loss in each oscillation cycle, respectively. So, the Q factor is defined as $Q = 2\pi E_{\text{ext}}/\Delta E_{\text{ext}}$ [30]. The theoretical Q factor range, 50–400, closely coincides with the empirical Q factor range, 50–800, found in the previous work [18].

Our simulations show that telescoped multi-walled CNT resonators are applicable to an ultra-high-frequency tuner, and such a gigahertz tuner can facilitate the development of high-frequency mechanical nanodevices such as fast scanning probe microscopes, magnetic resonance force microscopes and mechanical supercomputers [30]. The mechanical quality factor also plays a very important role in determining the sensitivity of NEMS-based devices. One can expect that the Q-factor will be greatly decreased by an increasing temperature such as the study on a cantilevered CNT beam oscillator in the previous work [30]. Therefore, further work should include MD simulations carried out at a temperature range substantially higher than 1 K (this work) to consider thermal dissipation because experiments are most likely to be conducted at temperatures much larger than 1 K.

5. Summary

We presented the schematics of a gigahertz tuner, which can be used repeatedly, based on a telescoped multi-walled CNT. The fixed short outer nanotube rigidly confines the longer inner nanotube, which can be freely telescoped, and then the desired resonance frequency can be achieved by controlling the cantilevered length of the inner nanotube. The dynamic operations of such a tuner were investigated via classical MD simulations based on a double-walled CNT. By adjusting the telescoped cantilevered length of a double-walled CNT, its resonance frequency can be matched to one of the signal frequencies and the telescoped cantilevered nanotube can be tuned to its resonance frequency. Our classical MD simulations showed that the telescoped cantilevered multi-walled CNT can be considered as an important component for a gigahertz tuner or bandpass filter, fast scanning probe microscopes and mechanical supercomputers.

Acknowledgement

This work was supported by the National Research Foundation of Korea Grant funded by the Korean Government (2009-0067884).

References

[1] S. Iijima, *Helical microtubules of graphitic carbon*, Nature 354 (1991), pp. 56–58.
[2] W.A. Goddard, D.W. Brenner, S.E. Lyshevski, and G.J. Iagrate (eds.), *Handbook of Nanoscience, Engineering, and Technology*, CRC Press, New York, 2003.
[3] D. Dian, G.J. Wagner, W.K. Liu, M.-Y. Yu, and R.S. Ruoff, *Mechanics of carbon nanotubes*, Appl. Mech. Rev. 55 (2002), pp. 495–532.
[4] J. Cumings and A. Zettl, *Low-friction nanoscale linear bearing realized from multiwall carbon nanotubes*, Science 289 (2000), pp. 602–604.
[5] J. Cumings and A. Zettl, *Localization and nonlinear resistance in telescopically extended nanotubes*, Phys. Rev. Lett. 93 (2004), 086801.
[6] Q. Zheng and Q. Jiang, *Multiwalled carbon nanotubes as gigahertz oscillators*, Phys. Rev. Lett. 88 (2002), 045503.
[7] S.B. Legoas, V.R. Coluci, S.F. Braga, P.Z. Coura, S.O. Dantas, and D.S. Galvão, *Molecular-dynamics simulations of carbon nanotubes as gigahertz oscillators*, Phys. Rev. Lett. 90 (2003), 055504.
[8] Y. Dai, W. Guo, C. Li, and C. Tang, *Ultrahigh frequency longitudinal oscillators from single-walled carbon nanotubes*, J. Comput. Theor. Nanosci. 5 (2008), pp. 1372–1376.
[9] Z. Qin, J. Zou, and X.-Q. Feng, *Influence of water on the frequency of carbon nanotube oscillators*, J. Comput. Theor. Nanosci. 5 (2008), pp. 1403–1407.
[10] J. Zhang, Y. Liu, M. Liu, W.M. Lau, and J. Yang, *Modeling of nanotube based nanopumps, nanoactuators and nanooscillators using lattice Boltzmann method*, J. Comput. Theor. Nanosci. 5 (2008), pp. 1440–1444.
[11] Z. Xu, *Energy dissipation in the double-walled carbon nanotube based mechanical oscillators*, J. Comput. Theor. Nanosci. 5 (2008), pp. 655–658.
[12] V. Sazonova, Y. Yaish, H. Ustunel, D. Roundy, T.A. Arias, and P.L. McEuen, *A tunable carbon nanotube electromechanical oscillator*, Nature 431 (2004), pp. 284–287.
[13] J.W. Kang and Q. Jiang, *Electrostatically telescoping nanotube nonvolatile memory device*, Nanotechnology 18 (2007), 095705.
[14] P. Kim and C.M. Lieber, *Nanotube nanotweezers*, Science 286 (1999), pp. 2148–2150.
[15] T. Rueckes, K. Kim, E. Joselevich, G.Y. Tseng, C.-L. Cheung, and C.M. Lieber, *Carbon nanotube-based nonvolatile random access memory for molecular computing*, Science 289 (2000), pp. 94–97.
[16] C. Li and T.-W. Chou, *Mass detection using carbon nanotube-based nanomechanical resonators*, Appl. Phys. Lett. 84 (2004), pp. 5246–5248.
[17] S.T. Purcell, P. Vincent, C. Journet, and V.T. Binh, *Tuning of nanotube mechanical resonances by electric field pulling*, Phys. Rev. Lett. 89 (2002), 276103.
[18] K. Jensen, C. Girit, W. Mickelson, and A. Zettl, *Tunable nanoresonators constructed from telescoping nanotubes*, Phys. Rev. Lett. 96 (2006), 215503.
[19] K. Jensen, J. Weldon, H. Garcia, and A. Zettl, *Nanotube radio*, Nano Lett. 7 (2007), pp. 3508–3511.
[20] J.W. Kang, Y.G. Choi, J.H. Lee, O.K. Kwon, and H.J. Hwang, *Molecular dynamics simulations of carbon nanotube oscillators deformed by encapsulated copper nanowires*, Mol. Simul. 34 (2008), pp. 829–835.

[21] J.W. Kang and J.H. Lee, *Multi-walled carbon nanotube oscillator behavior analysis using classical molecular dynamics simulations*, J. Korean Phys. Soc. 53 (2008), pp. 646–651.
[22] K.O. Song, H.J. Hwang, Y.G. Choi, and J.W. Kang, *Molecular dynamics study on a telescoping carbon-nanotube-based gigahertz tuner*, J. Korean Phys. Soc. 55 (2009), pp. 549–553.
[23] J.W. Kang, O.K. Kwon, and J.H. Lee, *Multi-walled carbon nanotube oscillators as multi-frequency generators for nano embedded systems*, J. Comput. Theor. Nanosci. 5 (2008), pp. 290–293.
[24] J.W. Kang, C.S. Won, G.H. Ryu, and Y.G. Choi, *Molecular dynamics study on resonance characteristics of gigahertz carbon nanotube motor*, J. Comput. Theor. Nanosci. 6 (2009), pp. 178–186.
[25] J.W. Kang, J.H. Lee, K.-S. Kim, and Y.G. Choi, *Molecular dynamics simulation study on capacitive nano-accelerometer of telescoping carbon nanotubes*, Model. Simul. Mater. Sci. Eng. 17 (2009), 025011.
[26] J. Tersoff, *Empirical interatomic potential for silicon with improved elastic properties*, Phys. Rev. B 38 (1988), pp. 9902–9905.
[27] J. Tersoff, *Modeling solid-state chemistry: Interatomic potentials for multicomponent systems*, Phys. Rev. B 39 (1989), pp. 5566–5568.
[28] D.W. Brenner, *Empirical potential for hydrocarbons for use in simulating the chemical vapor deposition of diamond films*, Phys. Rev. B 42 (1990), pp. 9458–9471.
[29] Z. Mao, A. Garg, and S.B. Sinnott, *Molecular dynamics simulations of the filling and decorating of carbon nanotubules*, Nanotechnology 10 (1999), pp. 273–277.
[30] H. Jiang, M.-F. Yu, B. Liu, and Y. Huang, *Intrinsic energy loss mechanisms in a cantilevered carbon nanotube beam oscillator*, Phys. Rev. Lett. 93 (2004), 185501.